A dynamic regularized gradient model of the subgrid-scale scalar flux

By G. Balarac†, J. Le Sommer† AND A. Vollant†

Accurate prediction of a scalar advected by a turbulent flow is needed for various applications. In the framework of large-eddy simulation (LES), a subgrid-scale (SGS) model for the subgrid-scale scalar flux has to be used. A gradient model derived from Taylor series expansions of the filtering operation is a well-known approach to model SGS quantities. This model is known to lead to high correlation levels between the unknown term and the model. However, this type of model can not be used in practical LES because it does not lead to sufficient global energy transfer from the large to the small scales. In this work, we propose a regularization of the gradient model based on a physical interpretation of this model. We compare the regularized gradient model with classic models through a priori tests. It is found that the new proposed model associated with a dynamic procedure exhibits very good performances in comparison with the standard dynamic eddy diffusivity gradient models. To better evaluate the new dynamic procedure, we perform a posteriori (large-eddy simulation) tests, showing a substantial improvement for various scalar statistics predictions.

1. Introduction

Various applications need to solve a scalar equation simultaneously to the governing flow equations. In these applications, the scalar can represent the temperature field or the concentration of chemical species in combustion, mixing or heat transfer studies. Due to the large range of motion scales in turbulent flows, the direct numerical simulation (DNS) of realistic applications is not yet available because of high computational costs. To overcome this limitation, the large-eddy simulation (LES) technique proposes solving explicitly only the large scales of the flow and modeling the impact of the smallest scales on the large scales. This separation between resolved large scales and modeled small scales is performed by a filtering operation to obtain the large-scale resolved field, $\bar{f}$, from the turbulent field, f. For a passive scalar, Z, the filtered transport equation in incompressible flow is given by

$$\frac{\partial \bar{Z}}{\partial t} + \bar{u}_i \frac{\partial \bar{Z}}{\partial x_i} = D \frac{\partial^2 \bar{Z}}{\partial x_i^2} - \frac{\partial T_i}{\partial x_i}, \tag{1.1}$$

where $T_i = \overline{u_i Z} - \bar{u}_i \bar{Z}$ is the subgrid-scale (SGS) scalar flux, which has to be modeled to perform LES. Two major strategies are available for developing SGS models (Sagaut 2005): functional and structural strategies. The functional modeling strategy considers the action of the subgrid terms on the transported quantity and not the unknown term itself. It can introduce a dissipative term, for example, that has a similar effect but not necessarily the same spatial structure. Conversely, the structural modeling strategy consists of using the best approximation of the unknown SGS term by constructing it

† Grenoble-INP/CNRS/UJF-Grenoble 1, LEGI UMR 5519, Grenoble, F-38041, France

from the known structure of small-scales. In the LES of a passive scalar context, a typical functional model is to introduce an eddy diffusivity, D_T, to model the SGS scalar flux as $T_i = D_T \partial \bar{Z}/\partial x_i$. Moin *et al.* (1991) introduce a dynamic model for D_T, similar to the dynamic Smagorinsky model used to model the eddy viscosity (Germano *et al.* 1991). This dynamic eddy diffusivity model (DEDM) is defined as

$$T_i^{\mathrm{DEDM}} = D_T \frac{\partial \bar{Z}}{\partial x_i} = C\Delta^2 |\bar{S}| \frac{\partial \bar{Z}}{\partial x_i}, \tag{1.2}$$

where C is a coefficient coming from the dynamic procedure. Moin *et al.* (1991) show that the dynamic procedure greatly improves the results of the simulations. However, even if a correct dissipation level is modeled, DEDM is generally known to have a weak local correlation between the model and the SGS term (Clark *et al.* 1979). On the other hand, the gradient model (GM) is a typical structural model based on a Taylor series expansion of the filtering operation (Vreman *et al.* 1997):

$$T_i^{\mathrm{GM}} = \frac{\bar{\Delta}^2}{12} \frac{\partial \bar{u}_i}{\partial x_j} \frac{\partial \bar{Z}}{\partial x_j}. \tag{1.3}$$

This type of model is known to give a good approximation of the unknown term with a high correlation between the unknown term and the model in a priori tests (Clark *et al.* 1979). However, this type of model is unstable due to the incorrect prediction of the dissipation. A popular solution to overcome the limitations of both functional and structural models is to use a mixed model (Vreman *et al.* 1997; Fabre & Balarac 2011).

In this work, we propose to develop a model combining the advantage of both approaches: structural and functional models. The approach is based on a physical interpretation of the gradient model. We show that only the stretching effects of the resolved velocity field on the resolved scalar gradient lead to energy transfer from small to large scales (backscatter effect). A regularization of the gradient model is then proposed. From a priori tests, the regularized gradient model associated with a dynamic procedure exhibits very good performances. This new dynamic regularized gradient model is then tested in a posteriori (LES) tests. It is shown that the new model substantially improves the prediction of various scalar statistics in comparison with a classic dynamic eddy diffusivity model.

2. Physical interpretation: the energy transfer given by the gradient model

The starting point to propose a physical interpretation of the gradient model (GM) model is to decompose the velocity gradient as $\frac{\partial \bar{u}_i}{\partial x_j} = \bar{S}_{ij} + \bar{\Omega}_{ij}$, with $\bar{S}_{ij} = 1/2 \left(\frac{\partial \bar{u}_i}{\partial x_j} + \frac{\partial \bar{u}_j}{\partial x_i} \right)$ and $\bar{\Omega}_{ij} = 1/2 \left(\frac{\partial \bar{u}_i}{\partial x_j} - \frac{\partial \bar{u}_j}{\partial x_i} \right)$, the filtered strain rate tensor and the filtered rotation rate tensor, respectively. The gradient model can thus be rewritten as

$$T_i^{\mathrm{GM}} = \frac{\bar{\Delta}^2}{12} \left(\bar{S}_{ij} + \bar{\Omega}_{ij} \right) \frac{\partial \bar{Z}}{\partial x_j}. \tag{2.1}$$

Moreover, the filtered strain rate tensor is symmetric; it can be thus written as

$$\bar{S}_{ij} = \sum_{k=1}^{3} \lambda^{(k)} e_i^{(k)} e_j^{(k)}, \tag{2.2}$$

with $\lambda^{(k)}$ and $\vec{e}^{(k)}$ the k^{th} (real) eigenvalue and the unitary eigenvector of the filtered strain rate tensor, respectively. Finally, the gradient model can be written as

$$T_i^{\text{GM}} = \frac{\bar{\Delta}^2}{12}\left(\bar{S}_{ij}^{\oplus} + \bar{S}_{ij}^{\ominus} + \bar{\Omega}_{ij}\right)\frac{\partial \bar{Z}}{\partial x_j}, \tag{2.3}$$

with

$$\bar{S}_{ij}^{\ominus} = \sum_{k=1}^{3} \min(0, \lambda^{(k)}) e_i^{(k)} e_j^{(k)} \text{ and } \bar{S}_{ij}^{\oplus} = \sum_{k=1}^{3} \max(0, \lambda^{(k)}) e_i^{(k)} e_j^{(k)}.$$

The functional performance of a SGS scalar flux model is given by its capability to accurately reproduce the grid-scales/subgrid-scales (GS/SGS) transfer between the resolved scalar "energy," $\bar{Z}^2$, and the SGS scalar variance, $\overline{ZZ} - \bar{Z}\bar{Z}$. From the transport equation of $\bar{Z}^2$ (Jiménez *et al.* 2001)

$$\frac{\partial \bar{Z}^2}{\partial t} + \bar{u}_i \frac{\partial \bar{Z}^2}{\partial x_i} = D\frac{\partial^2 \bar{Z}^2}{\partial x_i^2} - 2D\frac{\partial \bar{Z}}{\partial x_i}\frac{\partial \bar{Z}}{\partial x_i} - 2\frac{\partial \bar{Z} T_i}{\partial x_i} + 2T_i\frac{\partial \bar{Z}}{\partial x_i}, \tag{2.4}$$

it appears that this transfer is controlled by the SGS scalar dissipation, $T_i \partial \bar{Z}/\partial x_i$. From the proposed decomposition of the gradient model Eq. (2.3), the SGS scalar dissipation predicted by this model can be rewritten as

$$T_i^{\text{GM}} \frac{\partial \bar{Z}}{\partial x_i} = \frac{\bar{\Delta}^2}{12}\left(\bar{S}_{ij} + \bar{\Omega}_{ij}\right)\frac{\partial \bar{Z}}{\partial x_j}\frac{\partial \bar{Z}}{\partial x_i} = \sum_{k=1}^{3} \lambda^{(k)} \left(\frac{\partial \bar{Z}}{\partial x_i} e_i^{(k)}\right)^2. \tag{2.5}$$

Indeed, it can be shown that $\bar{\Omega}_{ij}(\partial \bar{Z}/\partial x_j)(\partial \bar{Z}/\partial x_i) = 0$. Thus, the transfer given by the gradient model is only controlled by the sign of the eigenvalues of $\bar{S}_{ij}$ and the SGS dissipation predicted by the gradient model can be written as

$$T_i^{\text{GM}} \frac{\partial \bar{Z}}{\partial x_i} = \frac{\bar{\Delta}^2}{12}\left(\underbrace{\bar{S}_{ij}^{\oplus}\frac{\partial \bar{Z}}{\partial x_j}\frac{\partial \bar{Z}}{\partial x_i}}_{>0} + \underbrace{\bar{S}_{ij}^{\ominus}\frac{\partial \bar{Z}}{\partial x_j}\frac{\partial \bar{Z}}{\partial x_i}}_{<0}\right). \tag{2.6}$$

Since the negative eigenvalues correspond to the compressional effects and the positive eigenvalues correspond to stretching effects (Nomura & Post 1998), a physical interpretation of the gradient model can be thus performed in terms of compressional, stretching and rotational effects of the resolved velocity field on the resolved scalar gradient. The rotational effect does not lead to GS/SGS transfer. Conversely, the compressional effect leads to forward transfer (negative value of the SGS dissipation), whereas the stretching effect leads to back-scatter (positive value of the SGS dissipation).

3. Regularization of the gradient model

3.1. *Proposed regularizations*

The unstable behavior of the gradient model is due to an overestimation of transfers from the subgrid-scales to the grid scales (Vreman *et al.* 1996). To avoid this unstable behavior, our proposition is to neglect all of these inverse transfers. From the previous section, this can be done by neglecting the stretching effects. At this stage, two models can be proposed. The first one is obtained by keeping only the term allowing the direct energy transfer. This leads to the first regularized gradient model (noted RGM1), which

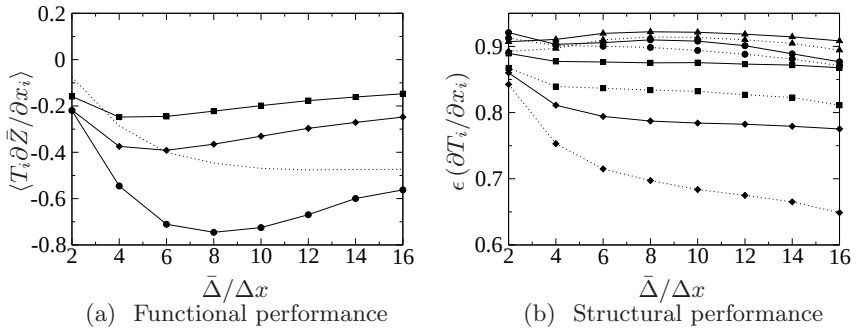

(a) Functional performance (b) Structural performance

FIGURE 1. (a) Mean SGS dissipation as a function of the filter width for the regularized gradient models (RGM, diamond), DEDM (circle), GM (square) and filtered DNS (dotted line). (b) Quadratic (solid line) and irreducible (dotted line) errors as a function of the filter width for RGM1 (diamond), RGM2 (triangle), DEDM (circle) and GM (square).

is written as

$$T_i^{\mathrm{RGM1}} = \frac{\bar{\Delta}^2}{12} \bar{S}_{ij}^{\ominus} \frac{\partial \bar{Z}}{\partial x_j}. \tag{3.1}$$

Another proposition is to neglect only the term $\bar{S}_{ij}^{\oplus}$ in the gradient model decomposition, Eq. (2.3). The second regularized gradient model (noted RGM2) is then written

$$T_i^{\mathrm{RGM2}} = \frac{\bar{\Delta}^2}{12} \left(\bar{S}_{ij}^{\ominus} + \bar{\Omega}_{ij} \right) \frac{\partial \bar{Z}}{\partial x_j}. \tag{3.2}$$

These two models differ only by keeping or not keeping the rotational effect. As already seen, the rotational effect does not influence the GS/SGS transfer instantaneously. These models will thus lead to the same GS/SGS transfer. Only the local approximation of the SGS scalar flux will be influenced by the rotational effect in the model formulation. This can be related to the bidimensional model proposed by Le Sommer *et al.* (2011) for ocean circulation simulations. Note also that this regularization approach is close to the approach proposed by Cottet & Wray (1997) for developing an anisotropic model for SGS shear stresses.

3.2. *Model performance measurements based on a priori tests*

The a priori tests are based on data extracted from direct numerical simulation (DNS) of a forced homogeneous isotropic turbulence. The DNS database is generated from a standard pseudo-spectral code and the simulation domain is discretized using 512^3 grid points on a domain of length 2π. A statistical steady flow is achieved by using a forcing term (Alvelius 1999), and the scalar field is initialized between 0 and 1 according to the procedure proposed by Eswaran & Pope (1988). The Schmidt number is taken equal to 0.7, and the Reynolds number based on the Taylor microscale is around 180 at the stationary state. The code and the flow configuration are similar to previous works where the modeling of the various SGS quantities were studied (Fabre & Balarac 2011; Balarac *et al.* 2008*a*,*b*). The DNS data are filtered in space to emulate LES quantities by using a spectral cut-off filter to reproduce the behavior of the spectral method employed in this work. Several filter sizes have been used, chosen as $2 \leq \bar{\Delta}/\Delta x \leq 16$, where $\bar{\Delta}$ is the filter width and Δx is the DNS mesh size.

The functional performance is studied first. As defined by Sagaut (2005), the functional

performance represents the ability of the model to reproduce the averaged effect of the SGS term on the transported quantity (here, the scalar field). As already discussed, in the context of LES of a passive scalar, the functional performance is the ability to predict the GS/SGS transfer, controlled by the SGS scalar dissipation, $T_i\partial\bar{Z}/\partial x_i$. Figure 1 (a) shows the mean SGS scalar dissipation, $\langle T_i\partial\bar{Z}/\partial x_i\rangle$, as a function of the filter width for various models. Note that RGM1 and RGM2 lead to the same SGS dissipation, noted RGM in the figure. The mean SGS scalar dissipation is negative, showing that the transfers are from the large (resolved) scales to the small ones. The GM under-predicts the magnitude of $\langle T_i\partial\bar{Z}/\partial x_i\rangle$ in comparison with the DNS results. This shows that this model does not provide enough dissipation. Conversely, the DEDM models are too dissipative with an over-prediction of the magnitude of $\langle T_i\partial\bar{Z}/\partial x_i\rangle$. The proposed regularization allows to improve the prediction of the mean SGS scalar dissipation by neglecting the inverse transfer, but the magnitude of the SGS scalar dissipation is still under-predicted. In the following section, a dynamic procedure will be proposed to improve this prediction. It is needed first to measure the structural performance of the regularized models to differentiate the performances of RGM1 and RGM2.

From Sagaut (2005), the structural performance is defined as the model's ability to describe locally the SGS unknown term appearing in the resolved equation. For the scalar, the SGS unknown term is the divergence of the SGS scalar flux, $\partial T_i/\partial x_i$, appearing in the scalar transport Eq. (1.1). The models' structural performance can be evaluated by using the notion of an optimal estimator introduced by Moreau *et al.* (2006) in the LES context. Considering f as the SGS term to model and g as a model of f based on a given set of variables ϕ, a quadratic error can be defined

$$\epsilon_{\mathrm{Q}} = \langle (f - g(\phi))^2 \rangle. \tag{3.3}$$

The concept of optimal estimator forecasts that any model g built on the set of variables ϕ will have a quadratic error higher than a minimal value, ϵ_{irr}, defined as

$$\epsilon_{irr} = \langle (f - \langle f|\phi\rangle)^2 \rangle \leq \epsilon_{\mathrm{Q}}, \tag{3.4}$$

where $\langle f|\phi\rangle$ is the expectation of the exact quantity f conditioned with the set of variables ϕ. The quantity $\langle f|\phi\rangle$ is thus called the optimal estimator of f for the set of variable ϕ, and the minimal error, ϵ_{irr}, is called the irreducible error. Optimal estimator theory allows to know to what extent a model based on a set of variables can be improved. Indeed, if the quadratic error of a given model is much higher than its irreducible part, an improvement can be expected. This concept has already been used to improve the modeling of SGS quantities (Balarac *et al.* 2008*a*,*b*; Fabre & Balarac 2011). The optimal estimator tool is now used to measure the structural performance of various models. Figure 1 (b) shows the evolution of the quadratic error, Eq. (3.3), and the irreducible error, Eq. (3.4), with the filter size. The errors are normalized by the statistical variance of the exact SGS term. As expected the GM quadratic error is smaller than DEDM quadratic error. Moreover, the DEDM irreducible error is always higher than the GM quadratic error. This shows that the improvement of the structural performance of DEDM can not be expected without adding new quantities to its set of variables. For both proposed regularized gradient models (RGM1 and RGM2), the performances are very different. RGM1 has good structural performance compared to RGM2. Indeed, the RGM2 irreducible error is even higher than the DEDM quadratic error, showing that this model proposition does not allow an improvement in comparison with a classic eddy diffusivity model. Conversely, RGM1 performs even better than GM, with the RGM1 quadratic

error smaller than the GM irreducible error, showing that we can not expect the same performance with the classic gradient model. However, an improvement can be expected for this model because the gap between the RGM1 quadratic error and its associated irreducible error is still important. Our proposition is to keep the RGM1 formulation (3.1) to regularize the gradient model and to propose a dynamic procedure for computing the model coefficient. The dynamic procedure is expected to improve the functional performance of the model, with a better evaluation of the mean SGS scalar dissipation and the structural performance with a quadratic error closer to the irreducible error.

3.3. *Dynamic procedure for the proposed regularized gradient model*

In the previous section, the RGM1 performance was measured by keeping a static coefficient coming from a Taylor series expansion. In this section, a dynamic procedure is now proposed to improve the model's performance. The regularized gradient model is thus re-written as

$$T_i^{\mathrm{RGM1}} = C\bar{\Delta}^2 \bar{S}_{ij}^{\ominus} \frac{\partial \bar{Z}}{\partial x_j}, \tag{3.5}$$

with C a coefficient to evaluate. The dynamic procedure uses a test filter (noted $\hat{\cdot}$), with a filter size such as $\hat{\Delta} = 2\bar{\Delta}$. Before describing the dynamic procedure, the mathematical derivation of the gradient model can be first recalled. The starting point is to write a Taylor series expansion for the filtering operation to evaluate $\overline{u_i Z}$ as function of $\bar{u}_i$ and $\bar{Z}$ (see Bedford & Yeo 1993, for details). This leads to (keeping only the first term of the Taylor series),

$$\overline{u_i Z} = \bar{u}_i \bar{Z} + \frac{\bar{\Delta}^2}{12} \frac{\partial \bar{u}_i}{\partial x_j} \frac{\partial \bar{Z}}{\partial x_j} + \mathcal{O}(\bar{\Delta}^4). \tag{3.6}$$

The gradient model is obtained by neglecting the terms with an order higher than $\bar{\Delta}^2$ in the RHS.

The proposed dynamic procedure is based on similar Taylor series expansions applied at the test filter level as already done in previous works (Balarac *et al.* 2008*a*; Fabre & Balarac 2011). The Taylor series expansion of the test filter for f and g, both quantities describing flow fields, leads to

$$\widehat{fg} - \hat{f}\hat{g} = \frac{\hat{\Delta}^2}{12} \frac{\partial \hat{f}}{\partial x_j} \frac{\partial \hat{g}}{\partial x_j} + \mathcal{O}(\hat{\Delta}^4). \tag{3.7}$$

By taking, $f = \bar{u}_i$ and $g = \bar{Z}$, Eq. (3.7) is written

$$\widehat{\bar{u}_i \bar{Z}} - \hat{\bar{u}}_i \hat{\bar{Z}} = \frac{\hat{\Delta}^2}{12} \frac{\partial \hat{\bar{u}}_i}{\partial x_j} \frac{\partial \hat{\bar{Z}}}{\partial x_j} + \mathcal{O}(\hat{\Delta}^4). \tag{3.8}$$

Now, neglecting the terms with an order higher than $\hat{\Delta}^2$ and using the proposed regularization with the same dynamic coefficient, the model at the test filter level can be written

$$\widehat{\bar{u}_i \bar{Z}} - \hat{\bar{u}}_i \hat{\bar{Z}} = C\hat{\Delta}^2 \hat{\bar{S}}_{ij}^{\ominus} \frac{\partial \hat{\bar{Z}}}{\partial x_j}. \tag{3.9}$$

This defines a relation between the Leonard-type term, $\widehat{\bar{u}_i \bar{Z}} - \hat{\bar{u}}_i \hat{\bar{Z}}$, and other quantities available in LES. This relation can thus be used to compute the model coefficient C. Assuming C is constant over homogeneous directions, it can be evaluated from a least-squares approximation according to the method proposed by Lilly (1992).

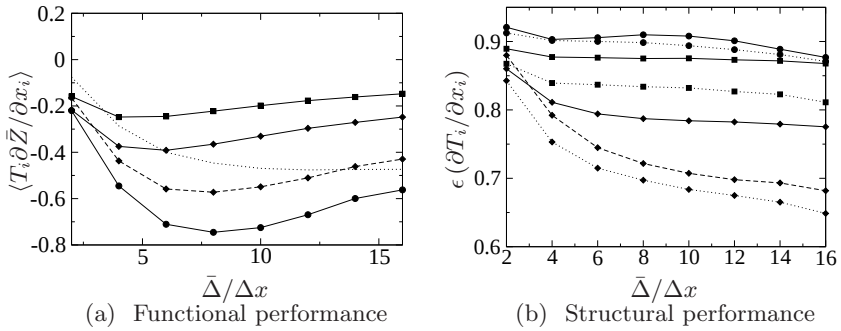

(a) Functional performance (b) Structural performance

FIGURE 2. (a) Mean SGS dissipation as a function of the filter width for RGM (solid line with diamond), DRGM (dashed line with diamond), DEDM (circle), GM (square) and filtered DNS (dotted line). (b) Quadratic (solid line) and irreducible (dotted line) errors as a function of the filter width for RGM (solid line with diamond), DRGM (dashed line with diamond), DEDM (circle) and GM (square).

The dynamic regularized gradient model (DRGM) performances are now measured and compared with the dynamic eddy diffusivity mode (DEDM), the gradient model (GM) and the static regularized model, Eq. (3.1), now noted RGM. Figure 2 (b) shows the comparison of the model errors. Note that DRGM and RGM have the same irreducible errors because these models are based on the same set of variables. The DRGM quadratic errors are the smallest quadratic errors, showing the improvement allowed by the dynamic procedure. This shows a significant improvement of the structural performance of the regularized model in comparison with the static formulation. Moreover, the DRGM quadratic error stays close to its irreducible errors, showing that it will be difficult to improve the model without adding new variables.

The functional performance can also been studied, Figure 2 (a). The improvement of the functional performance of the dynamic procedure is characterized by an increasing of the SGS scalar dissipation magnitude for DRGM. This allows us to correct the underprediction of the GS/SGS transfer observed with RGM.

4. A posteriori (LES) tests

The models are now tested by performing LES. The LES results will then be compared with the DNS filtered results. Note that in these test cases, the velocity field is still solved by DNS. Thus, when the LES data are compared with the filtered DNS data, the difference will only be due to the model used for the SGS scalar flux. The forced homogeneous isotropic turbulence test case is similar to the ones used in the a priori tests. Two LES meshes are used to investigate the performance of the models: 64^3 and 32^3 grid points.

Figure 3 shows the time evolution of the LES resolved scalar variance, $\langle \bar{Z}'^2 \rangle = \langle \bar{Z}\bar{Z} \rangle - \langle \bar{Z} \rangle \langle \bar{Z} \rangle$. The LES resolved scalar variance is compared with the variance of the filtered scalar field coming from the DNS data. The DNS scalar variance (without filtering), $\langle Z'^2 \rangle$, is also shown for comparison. In both cases, the same observations can be done about the model's performance. First, the DEDM resolved scalar variance is always notably smaller than the filtered DNS scalar variance. This is due to an over-prediction of the SGS dissipation with this model as already found in a priori tests. Conversely, the GM

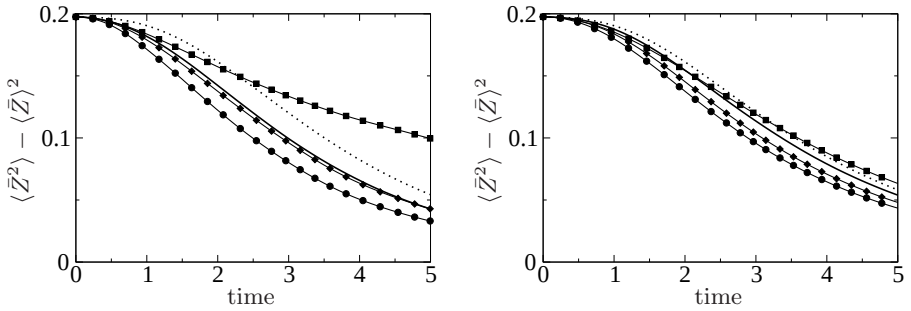

(a) $Sc = 0.7$; 32^3 grid points (b) $Sc = 0.7$; 64^3 grid points

FIGURE 3. Evolution of the LES resolved scalar variance, $\langle \bar{Z}'^2 \rangle$, with time for GM (square), DEDM (circle) and DRGM (diamond). The filtered (solid line) and no-filtered (dotted line) DNS scalar variances are also shown for comparison.

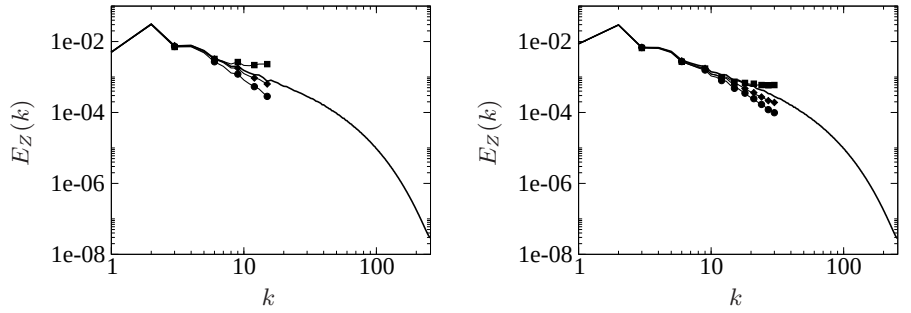

(a) $Sc = 0.7$; 32^3 grid points (b) $Sc = 0.7$; 64^3 grid points

FIGURE 4. Scalar variance spectrum, $E_Z(k)$, when $\langle \bar{Z}'^2 \rangle \approx 0.1$ for GM (square), DEDM (circle), DRGM (diamond) and DNS (solid line).

resolved scalar variance can be even higher than the DNS (no-filtered) scalar variance. This is due to a large under-prediction of the SGS dissipation. As expected, DRGM allows us to correct this behavior with a resolved scalar variance always smaller than the DNS scalar variance and close to the filtered scalar variance.

For further analysis, the scalar variance spectrum is shown in Figure 4. As expected, GM leads to an over-prediction of the scalar variance spectrum at the smallest resolved scales (highest resolved wave numbers). This characterizes the generation of non-physical fluctuations due to an over-estimation of the back-scatter effect. Conversely, DEDM under-predicts the scalar variance spectrum at the smallest resolved scales. This is due to the over-prediction of the SGS dissipation at these scales. DRGM allows the correction of these behaviors and stays close to the DNS, even for very coarse LES, Fig. 4 (a).

Finally, the influence of the SGS scalar flow model can be studied from additional statistics. First, the scalar probability density function (PDF) is shown in Figure 5 (a). The consequences of the SGS scalar flux model performance can then be observed on the local mixing prediction. The over-dissipation predicted by DEDM implies an over-estimation of the mixing process with higher PDF values of the portion of fully mixed

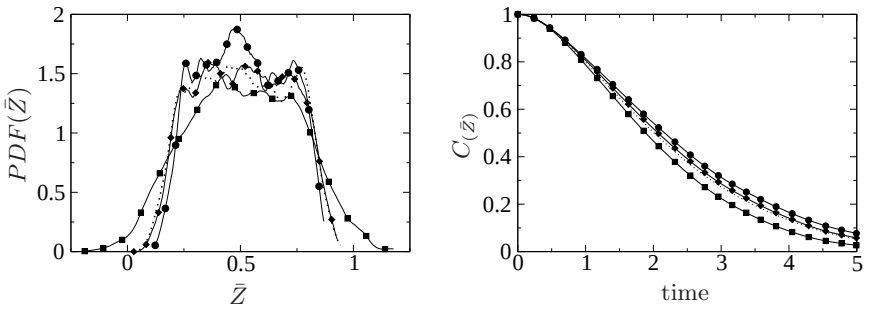

(a) Probability density function (b) Time correlation

FIGURE 5. (a) Probability density function (PDF) of the LES resolved scalar when $\langle \bar{Z}'^2 \rangle \approx 0.1$. (b) Time correlation of the LES resolved scalar, $C_{(\bar{Z})}$, computed by Eq. (4.1). GM (square), DEDM (circle), DRGM (diamond) and filtered DNS (dotted line).

fluid, $\bar{Z} \approx 0.5$, than the filtered DNS. Moreover, the unstable behavior of GM is characterized by unphysical values of $\bar{Z}$. Indeed, for this model, there are non zero probabilities of finding $\bar{Z} < 0$ or $\bar{Z} > 1$, whereas the scalar has to be bounded between its initial values, 0 and 1. The new proposed model allows the correction of this behavior. Finally, the time correlation of the LES resolved scalar can be studied. A SGS model has to model the contribution to temporal decorrelation of the subgrid-scales (He *et al.* 2002). The time auto-correlation of the LES resolved scalar is defined as

$$C_{(\bar{Z})}(t) = \frac{\langle \bar{Z}'(\vec{x}, t_0)\bar{Z}'(\vec{x}, t)\rangle}{\left(\langle \bar{Z}'^2(\vec{x}, t_0)\rangle \langle \bar{Z}'^2(\vec{x}, t)\rangle\right)^{1/2}}. \tag{4.1}$$

Figure 5 (b) shows the evolution of $C_{(\bar{Z})}$ for the different LES and for filtered DNS data. DRGM leads to better agreement. Indeed, DEDM lead to higher correlations whereas GM predicts faster decorrelation than the other models.

5. Conclusion

The gradient model is a well-known approach for modelling SGS quantities, such as the SGS scalar flux. However, this type of model can not be used in practical LES because it does not lead to enough global energy transfer from large to small scales. In this work, a physical interpretation of this model is first proposed in terms of compressional, stretching and rotational effects of the resolved velocity field on the resolved scalar gradient. The rotational effect is found to lead only to SGS diffusive effect. The compressional effect leads to forward scales transfer, whereas the stretching effect leads to back-scatter. A regularization is then proposed by neglecting the stretching effect in the model formulation. It is found that the new proposed model associated with a dynamic procedure exhibits very good performance in comparison with a standard dynamic eddy diffusivity model and the standard gradient model.

Acknowledgments

This work is supported by the Agence Nationale pour la Recherche (ANR) under Contract No. ANR-2010-JCJC-091601. Computing resources were provided by IDRIS-CNRS. The authors have benefited from fruitful discussions with CTR summer program participants.

REFERENCES

Alvelius, K. 1999 Random forcing of three-dimensional homogeneous turbulence. *Phys. Fluids* **11**, 1880–1889.

Balarac, G., Pitsch, H. & Raman, V. 2008*a* Development of a dynamic model for the subfilter scalar variance using the concept of optimal estimators. *Phys. Fluids* **20** (3), 1–8.

Balarac, G., Pitsch, H. & Raman, V. 2008*b* Modeling of the subfilter scalar dissipation rate using the concept of optimal estimators. *Phys. Fluids* **20** (9), 1–4.

Bedford, K. W. & Yeo, W. K. 1993 Conjective filtering procedures in surface water flow and transport. *Large Eddy Simulation of Complex Engineering and Geophysical Flows*, edited by B. Galperin, and S. A. Orszag, Cambridge Univ. Press, New York.

Clark, R. A., Ferziger, J. H. & Reynolds, W. C. 1979 Evaluation of subgrid-scale models using an accurately simulated turbulent flow. *J. Fluid Mech.* **91**, 1–16.

Cottet, G.-H. & Wray, A. A. 1997 Anisotropic grid-based formulas for subgrid-scale models. *Annual Research Brief, CTR, Stanford Univ.* pp. 113–122.

Eswaran, V. & Pope, S. 1988 Direct numerical simulations of the turbulent mixing of a passive scalar. *Phys. Fluids* **31**, 506–520.

Fabre, Y. & Balarac, G. 2011 Development of a new dynamic procedure for the clark model of the subgrid-scale scalar flux using the concept of optimal estimator. *Phys. Fluids* **23** (11), 1–11.

Germano, M., Piomelli, U., Moin, P. & Cabot, W. H. 1991 A dynamic subgrid-scale eddy viscosity model. *Phys. Fluids A* **3**, 1760–1765.

He, G., Rubinstein, R. & Wang, L.-P. 2002 Effects of subgrid-scale modeling on time correlations in large eddy simulation . *Phys. Fluids* **14**, 3186–2193.

Jiménez, C., Ducros, F., Cuenot, B. & Bédat, B. 2001 Subgrid scale variance and dissipation of a scalar field in large eddy simulations. *Phys. Fluids* **13**, 1748–1754.

Le Sommer, J., dOvidio, F. & Madec, G. 2011 Parameterization of subgrid stirring in eddy resolving ocean models. part 1: Theory and diagnostics. *Ocean Modelling* **39**, 154–169.

Lilly, D. 1992 A proposed modification of the Germano subgrid-scale closure method. *Phys. Fluids A* **4**, 633–635.

Moin, P., Squires, K., Cabot, W. & Lee, S. 1991 A dynamic subgrid-scale model for compressible turbulence and scalar transport. *Phys. Fluids A* **3**, 2746–2757.

Moreau, A., Teytaud, O. & Bertoglio, J. P. 2006 Optimal estimation for large-eddy simulation of turbulence and application to the analysis of subgrid models. *Phys. Fluids* **18**, 1–10.

Nomura, K. K. & Post, G. K. 1998 The structure and dynamics of vorticity and rate of strain in incompressible homogeneous turbulence. *J. Fluid Mech.* **377**, 65–97.

Sagaut, P. 2005 *Large eddy simulation for incompressible flows : an introduction (Third Edition)*. Springer.

Vreman, B., Geurts, B. & Kuerten, H. 1996 Large eddy simulation of the temporal mixing layer using the clark model. *Theor. Comput. Fluid Dyn.* **8**, 309–324.

Vreman, B., Geurts, B. & Kuerten, H. 1997 Large-eddy simulation of the turbulent mixing layer. *Journal of Fluid Mechanics* **339**, 357–390.